AIP | Physics of Fluids

Curvature suppresses the Rayleigh-Taylor instability

Philippe H. Trinh, Hyoungsoo Kim, Naima Hammoud, Peter D. Howell, S. Jonathan Chapman, and Howard A. Stone

Citation: Physics of Fluids (1994-present) **26**, 051704 (2014); doi: 10.1063/1.4876476
View online: http://dx.doi.org/10.1063/1.4876476
View Table of Contents: http://scitation.aip.org/content/aip/journal/pof2/26/5?ver=pdfcov
Published by the AIP Publishing

PHYSICS OF FLUIDS **26**, 051704 (2014)

Curvature suppresses the Rayleigh-Taylor instability

Philippe H. Trinh,[1,a)] Hyoungsoo Kim,[2,b)] Naima Hammoud,[3]
Peter D. Howell,[1] S. Jonathan Chapman,[1] and Howard A. Stone[2,a)]
[1]*Oxford Centre for Industrial and Applied Mathematics, Mathematical Institute, University of Oxford, Oxford OX2 6GG, United Kingdom*
[2]*Department of Mechanical and Aerospace Engineering, Princeton University, Princeton, New Jersey 08544, USA*
[3]*Program in Applied and Computational Mathematics, Princeton University, Princeton, New Jersey 08544, USA*

(Received 20 January 2014; accepted 4 April 2014; published online 20 May 2014)

The dynamics of a thin liquid film on the underside of a curved cylindrical substrate is studied. The evolution of the liquid layer is investigated as the film thickness and the radius of curvature of the substrate are varied. A dimensionless parameter (a modified Bond number) that incorporates both geometric parameters, gravity, and surface tension is identified, and allows the observations to be classified according to three different flow regimes: stable films, films with transient growth of perturbations followed by decay, and unstable films. Experiments and linear stability theory confirm that below a critical value of the Bond number curvature of the substrate suppresses the Rayleigh-Taylor instability. © *2014 AIP Publishing LLC*. [http://dx.doi.org/10.1063/1.4876476]

When a dense fluid is accelerated into a fluid of lower density, the interface between the two fluids becomes unstable. For over a century, the gravitational version of this problem – the Rayleigh-Taylor instability – has been studied extensively, both experimentally and theoretically,[1–3] because the phenomenon is ubiquitous in nature and technology.[4–6] In general, these studies of gravitationally driven instabilities are performed in a planar geometry that is either horizontal or inclined.[7–9] Here we study the Rayleigh-Taylor instability in a curved geometry and identify conditions where the curvature of the substrate suppresses the instability.

One application for film flow on a curved surface concerns the development of plasma-facing components for fusion energy reactors. In such systems it is necessary to protect the plasma and the container wall from each other. It has been suggested that a film of liquid metal offers many advantages over solids as a plasma-facing material.[10,11] For such a system to be successful, it must operate in a regime where the film flowing along the underside of the curved surface remains stable.

Although most studies of thin film dynamics have considered flow along a planar substrate, there is a small literature where the ideas are developed for curved substrates. Such studies include the temporal evolution of two-dimensional thin liquid films, which exhibit thinning of the interface near regions of large curvature,[12] the flow along the interior surface of a cylindrical tube with a weakly curved centerline,[13] and the flow inside a rotating horizontal cylinder, e.g., Refs. 14–16. A general set of equations for viscous flow of a thin film along a curved substrate was proposed by Roy *et al.*[17] and Howell,[18] where the latter identified three distinguished limits, depending on whether an appropriate dimensionless curvature of the substrate is small, nearly constant, or large (see also Ref. 19).

In this letter, we study experimentally and theoretically the hydrodynamic stability of a suspended thin liquid film under a curved surface. We use the thin-film equations, well-known from viscous flow theory, to provide a description of the role of substrate curvature on the gravitationally

[a)]Authors to whom correspondence should be addressed. Electronic mail: trinh@maths.ox.ac.uk and hastone@princeton.edu.
[b)]P. H. Trinh and H. Kim contributed equally to this work.

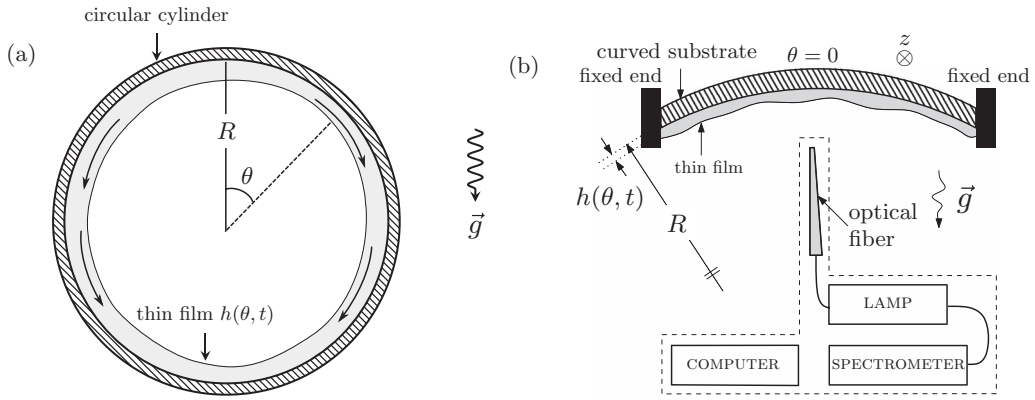

FIG. 1. (a) Thin film flow on a circular cylinder and (b) schematic of the experimental setup. The substrate is formed from a curved sheet with the axial direction (z) directed into the page.

driven flow of the film on the underside of a circular cylinder (Fig. 1(a)). These equations are solved analytically in the crucial regime near the top of the cylinder. The analytical predictions are confirmed by numerical solutions of the full equations. In addition, we perform experiments to measure the evolution of the thin film shape for different aspect ratios between the film thickness and the radius of curvature of the substrate formed from a curved sheet (Fig. 1(b)). Based upon the equations, we identify a single dimensionless parameter $B = \rho g R h_i/\gamma$, a modified Bond number that governs the behaviour of the flow and incorporates the surface tension γ, initial film thickness h_i, and substrate curvature R^{-1}, where ρ is the density of the fluid and g is the gravitational acceleration. Below a critical value of B, the film is stable to perturbations with a thickness that decreases monotonically in time. For larger values of B, i.e., thicker films (or flatter substrates), the dynamics exhibit either transient perturbation growth followed by decay, or instability via drop formation. The combination of theory and experiments provides a relatively complete characterization of the Rayleigh-Taylor instability of a liquid layer under a curved surface, and the manner in which substrate curvature can stabilize the film.

We consider the flow of a thin liquid film initially placed on the underside of a curved substrate. Here, we focus on the two-dimensional case where the substrate is cylindrical with constant curvature, $1/R > 0$ (Fig. 1(a), left). However, the following theory is local in nature, and so is applicable to any 2D substrate geometry with a local maximum and non-singular curvature. The film thickness is denoted $h(\theta, t)$, with $\theta = 0$ at the maximum point of the substrate. For the limit $h/R \ll 1$, with subscripts denoting derivatives, the thin film equation on the underside of a cylindrical surface is (e.g., Refs. 8 and 20)

$$h_t + \frac{1}{3\mu R}\left[h^3\left(\frac{\gamma}{R}\kappa_\theta + \rho g\left(\frac{h_\theta \cos\theta}{R} + \sin\theta\right)\right)\right]_\theta = 0, \tag{1}$$

where μ is the liquid viscosity and $\kappa = R^{-2}(h_{\theta\theta} + h)$ is the leading-order mean curvature of the film, which accounts for the profile of the interface and the curvature of the substrate.

It is convenient to scale the film height by an initial average film thickness h_i and time by the gravitational relaxation scale $\mu R/\left(\rho g h_i^2\right)$. Then, Eq. (1) can be recast in dimensionless form as (we retain the same variables)

$$h_t + \frac{1}{3}\left[h^3\left(\frac{\delta^2}{B}\left(h_{\theta\theta\theta} + h_\theta\right) + \delta h_\theta \cos\theta + \sin\theta\right)\right]_\theta = 0, \tag{2}$$

where $\delta = h_i/R$ is the aspect ratio of the film and $B = \rho g R h_i/\gamma$ is the modified Bond number. For many applications we expect $\delta \ll 1$. We are now interested in examining the growth or decay of a perturbation of the initial uniform profile, $h(\theta, 0) = 1$. An example of such a profile, numerically computed using Eq. (2), is shown in Fig. 2(a) (the details are presented in the numerical discussion to follow). We note that at leading order as $\delta \to 0$, Eq. (2) is hyperbolic, and the characteristic

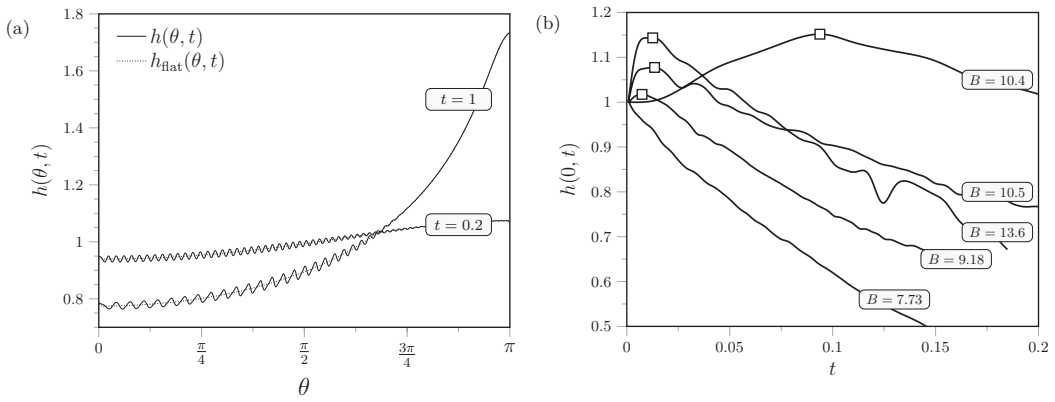

FIG. 2. (a) Numerical solutions, $h(\theta, t)$ (solid), of Eq. (2) at dimensionless times $t = 0.2$ and $t = 1$ for $B = 20$, $\delta = 10^{-3}$, and initial condition $h(\theta, 0) = 1 + D\sin(k^*\theta/\sqrt{\delta})$, where k^* is chosen to produce maximal perturbation growth and $D = 10^{-2}$ is a perturbation amplitude. The dotted lines correspond to $h_{\text{flat}}(\theta, t)$, the solution with $D = 0$. (b) Measurement of film thickness (re-scaled by h_i) as a function of non-dimensional time (re-scaled by $\mu R/(\rho g h_i^2)$) for various values of B. For $B > 8$, the maximal thickness is marked by a square.

projections in the (θ, t)-plane indicate that information propagates monotonically towards $\theta = \pi$ as time increases. We shall then focus on the region near the top of the cylinder ($\theta = 0$), where the gravitational instabilities are expected to be strongest. We derive an equation that describes the local behaviour of the film by setting $\theta = \delta^{1/2}x$. Keeping only the leading-order terms in Eq. (2) for $\delta \ll 1$, we obtain a simplified equation

$$h_t + \frac{1}{3}\left[h^3\left(B^{-1}h_{xxx} + h_x + x\right)\right]_x = 0. \tag{3}$$

Thus, where the destabilizing effect of gravity is expected to be the largest, only one dimensionless parameter, B, is significant. In the limit of zero surface tension, $B \to \infty$, Eq. (3) has the form of a backward diffusion equation, which is unconditionally unstable.

With the initial condition $h(x, 0) = 1$, then for any B, Eq. (3) has a solution $h_0(T) = T^{-1/2}$ where $T = 1 + \frac{2}{3}t$. This solution corresponds to gravitationally driven drainage with uniform thinning of the film. It is natural to consider the evolution of small perturbations to this uniform profile by setting $h = h_0(T)(1 + \epsilon\eta(x, T))$, where $\epsilon \ll 1$. From Eq. (3) and at leading order in ϵ, the perturbed shape, $\eta(x, T)$, satisfies

$$\eta_T + \frac{1}{2T^{3/2}}\left(B^{-1}\eta_{xxxx} + \eta_{xx}\right) + \frac{3}{2T}\left(x\eta_x + \tfrac{2}{3}\eta\right) = 0. \tag{4}$$

We consider an initial sinusoidal perturbation $\eta(x, 1) = e^{ikx}$ and solve Eq. (4) to find

$$\eta(x, T) = A(k, T)\exp\left(\frac{ikx}{T^{3/2}}\right), \tag{5}$$

$$A(k, T) = \frac{1}{T}\exp\left[\left(1 - T^{-7/2}\right)\frac{k^2}{7} - B^{-1}\left(1 - T^{-13/2}\right)\frac{k^4}{13}\right]. \tag{6}$$

For a given initial wave number, k, the amplitude factor $A(k, T)$ dictates the growth or decay of a perturbation as a function of B and time. A detailed analysis of this function establishes that η will either decay monotonically, or initially grow and decay afterwards. The initial behavior of the disturbance is given by

$$A(k, T) \sim 1 + \frac{\Delta}{2}(T - 1) \quad \text{as } T \to 1^+, \tag{7}$$

where $\Delta = k^2 - 2 - B^{-1}k^4$. By examining Δ, we see that for $B > 8$, there exist a band of wavenumbers $\sqrt{2} < k < \infty$ such that $\Delta > 0$. It is for these values of B that initial growth of the

perturbations occurs in Eq. (7); otherwise the perturbations all decay monotonically in time. Thus, we predict that there is a critical value of the Bond number, which relates the initial film height h_i and the substrate curvature $1/R$, such that the Rayleigh-Taylor instability is suppressed. According to Eq. (6), $A(k, T) \sim \text{const.}/T$ as $T \to \infty$, so eventually all (small) disturbances decay algebraically regardless of the initial wavenumber k.

In summary, the conclusions of the asymptotic analysis are: (i) any initial disturbance must immediately decay if $B < 8$ and (ii) for $B > 8$, although any disturbance must eventually decay according to the linearized theory, the initial transient growth may result in an amplification that is exponentially large in the wavenumber as $B \to \infty$. Also, as B increases, the growth of perturbations occurs over longer times and for larger wavenumbers k, resulting in a much higher amplitude. It should be expected that once B is no longer $O(1)$, the linearized analysis breaks down and we must turn to nonlinear analyses of stability. Next, we present, in turn, experimental and numerical results.

For the experiments, we use two silicone oils: one with density $\rho = 970$ kg/m^3, surface tension $\gamma = 18$ mN/m, and kinematic viscosity $\nu = 1000$ cS; the other one with density $\rho = 950$ kg/m^3, surface tension $\gamma = 19$ mN/m, and kinematic viscosity $\nu = 20$ cSt. We create substrate curvature by mechanically fixing two sides of a flexible polycarbonate sheet, as shown in Fig. 1(b). The curvature is adjusted by precise displacements of two linear stages installed at the edges of the deformable plate.

To make a uniform thin liquid film, we first coat silicone oil on top of the substrate by using a spin coater. Then, the liquid film layer is maintained on a horizontal table until the film thickness is uniform, which is validated by measurements with a confocal laser scanning microscope with fluorescent dye and an optical interferometry device. The error in the position of the horizontal axis of the aligned table is less than 0.1°, which is calibrated by a digital protractor (PRO3600).

When a uniform thin liquid layer is obtained, we impose a curvature to the substrate and turn it upside down. By varying the initial film thickness, h_i, of silicone oil and the curvature ($1/R$) of the substrate, we vary the aspect ratio in the range $2 \times 10^{-5} < \delta < 2.2 \times 10^{-3}$ and the modified Bond number in the range $4 < B < 164$.

To measure the evolution of the film thickness, we use an optical interferometry device (Fiber optic spectrometer, OceanOptics). The device is integrated with a light source (Tungsten halogen lamp, LS-1-LL) and a CCD array-based spectrometer, which measures wavelengths between 200–1100 nm. Due to the refractive index of the film, there is an optical path difference between the reflected and refracted wavelengths. By Snell's law, the path difference is $\cong 2n_f h$, where we can measure the dimensionless film thickness, $h(\theta, t)$, and n_f is a refractive index of the thin film; in our set-up the inclination angle of the light source is 90° ($\theta = 0$). Also, the refractive index of the silicone oil is 1.403 and the optical path is calculated by the optical interference pattern that is obtained from the spectrometer.

We measure the evolution of the film thickness at the center of the geometry ($\theta = 0$), as shown in the dashed box of Fig. 1(b). Typical measurements of the film thickness $h(0, t)$ for modest values of B are presented in Fig. 2(b). Based on the theoretical results, we expect that for $B < 8$, the film thickness near the top should decrease monotonically; this is demonstrated by, for example, the profile of $B = 7.73$ in Fig. 2(b). Indeed, other experimental results with $B < 8$ confirm similar behaviour: within this stable regime, the gravitational Rayleigh-Taylor instability is always suppressed due to the curvature of the substrate.

For values of $B > 8$, the theory predicts an initial transient growth of perturbations followed by eventual decay. This, too, is confirmed by the profiles of Fig. 2(b). Within this transient regime, we observe the formation of small droplets on the free surface, and their motion is followed by observing the side and top views using DSLR cameras (Nikon D5100 and D90 with AF-S DX Zoom-Nikkor 18-55mm f/3.5-5.6G lens). As shown in the side view of Fig. 3(b) (Multimedia view), the diameter of the sliding droplet is about 12 mm. These droplets slide in the angular direction, but remain attached to the interface (i.e., no dripping). Their size can be estimated by balancing surface tension and gravity, i.e., the typical dimension is $2\pi\sqrt{2}\ell_c$ where $\ell_c = \sqrt{\gamma/\rho g}$ is the capillary length. The sliding sessile droplet size is comparable with the wavelength of the fastest growing mode in the classical Rayleigh-Taylor instability problem.[7]

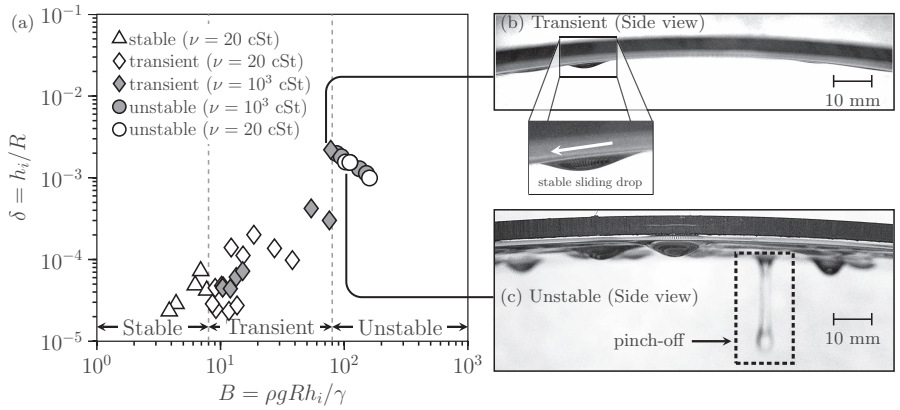

FIG. 3. (a) Experimental results in the (B, δ)-plane and classified as stable, transient, or unstable. Two critical values of the Bond number are indicated: $B = 8$ and $B = 80$. Experimental images of the side view in the case of (b) transient and (c) unstable flows. Videos of top and side views of transient flow can be seen in (b) and pinch-off in (c). (Multimedia view) [URL: http://dx.doi.org/10.1063/1.4876476.1] [URL: http://dx.doi.org/10.1063/1.4876476.2]

If we continue to increase B ($B > 80$ in the experiments), the thin film will destabilize. As shown in Fig. 3(c) (Multimedia view), this regime of large values of B is characterized by drops pinching off from the free surface. The diameter of all droplets is again about 12 mm. We further note that for $B > 15$, three dimensional effects were experimentally observed in the form of wave patterns in the axial direction (z), which can be seen in Fig. 3(b) (Multimedia view).

Thus we see that each experimental result can be classified as stable, transient, or unstable, and this is summarized in the (B, δ) phase plane shown in Fig. 3(a). We further note the $B = O(1)$ transition between curvature-stabilized dynamics and the classical Rayleigh-Taylor instability can be observed by balancing the time scale for drainage of the thin film, $O(\mu R/(\rho g h_i^2))$, with the time scale for growth of the Rayleigh-Taylor instability, which is $O(\mu\gamma/[(\rho g)^2 h_i^3])$ (de Gennes *et al.*,[21] p. 117).

We now seek to compare the asymptotic and experimental results to the numerical solutions of the full thin film problem in Eq. (2). This full problem is solved using finite differences beginning from an initial condition $h(\theta, 0) = 1 + D\sin(k^*\theta/\sqrt{\delta})$ and solved over $0 \le \theta \le \pi$, imposing symmetry conditions at $\theta = 0, \pi$. For $B \ge 8$, we choose k^* to be the wavenumber in Eq. (5) that produces maximal growth, where $\partial_k A = 0 = \partial_T A$; for $B < 8$, we choose $k^* = 2$ (its value at $B = 8$). We note that although the initial condition may not be symmetric at $\theta = \pi$, the hyperbolic nature of Eq. (2) ensures that the symmetry is imposed for $t > 0$ in a stable manner.

We then compute the difference

$$H(\theta, t) = \frac{1}{D}\left[h(\theta, t) - h_{\text{flat}}(\theta, t)\right], \tag{8}$$

where h_{flat} is the solution of Eq. (2) with an initial condition with no perturbation, $D = 0$. Numerical profiles of $h(\theta, t)$ and $h_{\text{flat}}(\theta, t)$ are shown in Fig. 2(a), and the corresponding differences, $H(\theta, t)$ are shown in Fig. 4. We see the decay of the initial sinusoidal perturbation (Fig. 4(a)) as the waves are advected towards the bottom of the cylinder (Fig. 4(b)).

To measure the magnitude of the perturbations over the upper half of the cylinder, for each choice of D, k^*, B, and δ, we use two measures: (i) the maximal perturbation, $\eta_{\max}(t) \equiv \max_{\theta \le \pi/2} H(\theta, t)$, or (ii) the average amplitude, $\eta_{\text{avg}}(t)$, of the oscillations in H for $\theta \le \pi/2$. The maximal values of $\eta_{\max}(t)$ or $\eta_{\text{avg}}(t)$ over all time are computed and compared with the maximal value of $A(k^*, t)$ over all time. The results are shown in Fig. 5, and demonstrate that the asymptotic prediction of Eq. (6) lies between the two measures of perturbation instability (for $\delta = 10^{-3}$ and $D = 10^{-2}$).

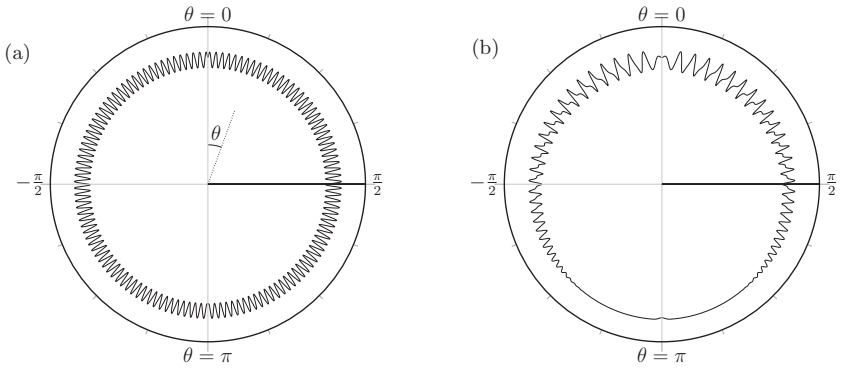

FIG. 4. Plots of $H(\theta, t) = \frac{1}{D}[h(\theta, t) - h_{\text{flat}}(\theta, t)]$ from Eq. (8) at times (a) $t = 0$ and (b) $t = 1$, showing the evolution of an initial sinusoidal disturbance on a thin film in a circular cylinder. The parameters are $B = 20$ and $\delta = 10^{-3}$, with initial condition $h(\theta, 0) = 1 + D\sin(k^*\theta/\sqrt{\delta})$ (same as Fig. 2(a)). The radial scaling of the two profiles has been exaggerated.

The numerical results agree favourably with the experimental measurements. The critical value of $B = 8$ can be identified clearly in asymptotic, numerical, and experimental results.

In summary, we have studied the gravitational Rayleigh-Taylor instability for a liquid film under a curved substrate. Using theoretical and experimental approaches, we identified two critical conditions to separate different flow regimes, and documented how a geometric feature, the substrate curvature, can suppress the Rayleigh-Taylor instability. Of course, there are other ways to suppress this instability, e.g., different external effects such as temperature gradients,[22] applied electric fields,[23] and mechanical forces.[24]

In addition to incorporating additional physics, we emphasize that the theoretical scope of this paper is only focused on linearized stability. Indeed, the transient growth observed for $B > 8$ may cause a sufficiently large perturbation of the free surface to trigger (nonlinear) instability. A weakly nonlinear analysis in such cases would then be needed to bridge the complex dynamics observed in the experiments and the numerics of Eq. (1).

It is also possible to extend our results to three-dimensional flow situations. For example, we would expect that for three-dimensional substrates where the local curvature is parabolic, the Rayleigh-Taylor instability is suppressed. However, nonlocal curvature gradients and other effects

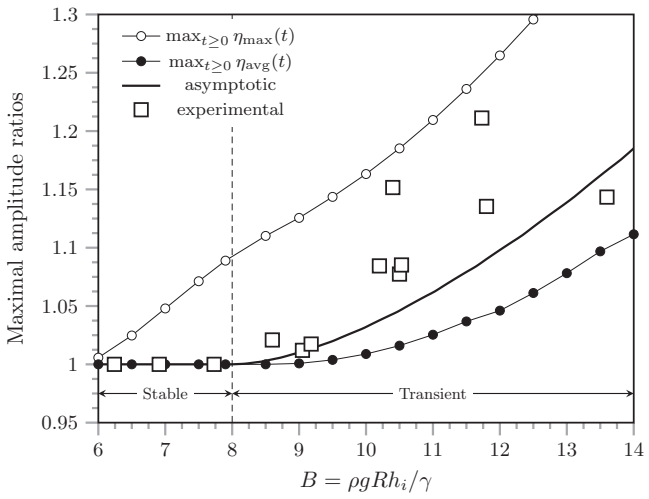

FIG. 5. Maximal amplitude ratios, $\eta_{\max}$ (top curve) and η_{avg} (bottom curve) over all time for the full problem in Eq. (2) with $\delta = 10^{-3}$, $D = 10^{-2}$, and $k = k^*$. The asymptotically predicted $\max_{t\geq 0} A(k^*, t)$ (thick line) lies between the two numerical results. The experimental results (squares) measure the maximum value of $h(0, t)/h(0, 0)$ (see Fig. 2).

of non-axisymmetric topographies (e.g., imposing inlet or outlet conditions for the draining process) may change the flow characteristics. These more general three-dimensional aspects are the subject of ongoing investigations.

We thank R. Goldston, M. Jaworski, R. Kaita, B. Koel, R. Majeski, and C. Skinner for helpful conversations about liquid walls as plasma-facing components, and also I. Jacobi for helping in the film thickness measurements. The DOE Fusion Energy Sciences Program is thanked for support of this research via Grant No. DE-SC0008598 to H.A.S. Finally, we gratefully acknowledge the Oxford-Princeton Collaborative Workshop Initiative for providing an opportunity for this collaborative work.

[1] G. I. Taylor, "The instability of liquid surfaces when accelerated in a direction perpendicular to their planes" Proc. R. Soc. London Ser. A **201**, 192–196 (1950).
[2] L. Rayleigh, "Investigation of the character of the equilibrium of an incompressible heavy fluid of variable density," Proc. London Math. Soc. **s1-14**(1), 170–177 (1882).
[3] P. G. Drazin and W. H. Reid, *Hydrodynamic Stability* (Cambridge University Press, Cambridge, 2004).
[4] D. H. Sharp, "An overview of Rayleigh-Taylor instability," Phys. D **12**, 3–18 (1984).
[5] J. D. Lindl and W. C. Mead, "Two-dimensional simulation of fluid instability in laser-fusion pellets," Phys. Rev. Lett. **34**, 1273 (1975).
[6] G. A. Houseman and P. Molnar, "Gravitational Rayleigh-Taylor instability of a layer with non-linear viscosity and convective thinning of continental lithosphere," Geophys. J. Intl. **128**, 125–150 (1997).
[7] M. Fermigier, L. Limat, J. E. Wesfreid, P. Boudinet, and C. Quilliet, "Two-dimensional patterns in Rayleigh-Taylor instability of a thin layer," J. Fluid Mech. **236**, 349–383 (1992).
[8] A. A. King, L. J. Cummings, S. Naire, and O. E. Jensen, "Liquid film dynamics in horizontal and tilted tubes: Dry spots and sliding drops," Phys. Fluids **19**, 042102 (2007).
[9] A. Indeikina, I. Veretennikov, and H.-C. Chang, "Drop fall-off from pendent rivulets," J. Fluid Mech. **338**, 173–201 (1997).
[10] R. Majeski, H. Kugel, R. Kaita, M. G. Avasarala, M. G. Bell, R. E. Bell, L. Berzak, P. Beiersdorfer, S. P. Gerhardt, E. Granstedt, T. Gray, C. Jacobson, J. Kallman, S. Kaye, T. Kozub, B. P. LeBlanc, J. Lepson, D. P. Lundberg, R. Maingi, D. Mansfield, S. F. Paul, G. V. Pereverzev, H. Schneider, V. Soukhanovskii, T. Strickler, D. Stotler, J. Timberlake, L. E. Zakharov, The NSTX and LTX Research Teams, "The impact of lithium wall coatings on NSTX discharges and the engineering of the Lithium Tokamak eXperiment (LTX)," Fus. Eng. Des. **85**(7–9), 1283–1289 (2010).
[11] R. Kaita, L. Berzak, D. Boyle, T. Gray, E. Granstedt, G. Hammett, C. M. Jacobson, A. Jones, T. Kozub, H. Kugel, B. Leblanc, N. Logan, M. Lucia, D. Lundberg, R. Majeski, D. Mansfield, J. Menard, J. Spaleta, T. Strickler, J. Timberlake, J. Yoo, L. Zakharov, R. Maingi, V. Soukhanovskii, K. Tritz, and S. Gershman, "Experiments with liquid metal walls: Status of the lithium tokamak experiment," Fus. Eng. Des. **85**, 874–881 (2010).
[12] L. W. Schwartz and D. E. Weidner, "Modeling of coating flows on curved surfaces," J. Eng. Math. **29**, 91–103 (1995).
[13] O. E. Jensen, "The thin liquid lining of a weakly curved cylindrical tube," J. Fluid Mech. **331**, 373–403 (1997).
[14] H. K. Moffatt, "Behaviour of a viscous film on the outer surface of a rotating cylinder," J. Mech. **16**, 651–673 (1977).
[15] J. Ashmore, A. E. Hosoi, and H. A. Stone, "The effect of surface tension on rimming flows in a partially filled rotating cylinder," J. Fluid Mech. **479**, 65–98 (2003).
[16] E. S. Benilov, N. Kopteva, and S. B. G. O'Brien, "Does surface tension stabilize liquid films inside a rotating horizontal cylinder?" Q. J. Mech. Appl. Math. **58**, 185–200 (2005).
[17] R. V. Roy, A. J. Roberts, and M. E. Simpson, "A lubrication model of coating flows over a curved substrate in space," J. Fluid Mech. **454**, 235–261 (2002).
[18] P. D. Howell, "Surface-tension-driven flow on a moving curved surface," J. Eng. Math. **45**, 283–308 (2003).
[19] T. G. Myers, J. P. F. Charpin, and S. J. Chapman, "The flow and solidification of a thin fluid film on an arbitrary three-dimensional surface," Phys. Fluids **14**, 2788–2803 (2002).
[20] H. Ockendon and J. R. Ockendon, *Viscous Flow* (Cambridge University Press, Cambridge, 1995).
[21] P.-G. De Gennes, F. Brochard-Wyart, and D. Quéré, *Capillarity and Wetting Phenomena: Drops, Bubbles, Pearls, Waves* (Springer-Verlag, New York, 2004).
[22] J. M. Burgess, A. Juel, W. D. McCormick, J. B. Swift, and H. L. Swinney, "Suppression of dripping from a ceiling," Phys. Rev. Lett. **86**, 1203 (2001).
[23] N. A. Bezdenezhnykh, V. A. Briskman, A. A. Cherepanov, and M. T. Sharov, "Control of the stability of liquid surfaces by means of variable fields," Fluid Mech. Sov. Res. **15**, 11–32 (1986).
[24] G. H. Wolf, "Dynamic stabilization of the interchange instability of a liquid-gas interface," Phys. Rev. Lett. **24**, 444 (1970).